Merkel cell polyomavirus-negative Merkel cell carcinoma originating from in situ squamous cell carcinoma: a keratinocytic tumor with neuroendocrine differentiation

Thibault Kervarrec, Silke Appenzeller, Mahtab Samimi, Bhavishya Sarma, Eva-Maria Sarosi, Patricia Berthon, Yannick Le Corre, Ewa Hainaut-Wierzbicka, Astrid Blom, Nathalie Benethon, et al.

▶ **To cite this version:**

Thibault Kervarrec, Silke Appenzeller, Mahtab Samimi, Bhavishya Sarma, Eva-Maria Sarosi, et al.. Merkel cell polyomavirus-negative Merkel cell carcinoma originating from in situ squamous cell carcinoma: a keratinocytic tumor with neuroendocrine differentiation. Journal of Investigative Dermatology, 2022, 142 (3), pp.516-527. 10.1016/j.jid.2021.07.175 . hal-03385922

HAL Id: hal-03385922
https://hal.inrae.fr/hal-03385922

Submitted on 22 Jul 2024

HAL is a multi-disciplinary open access archive for the deposit and dissemination of scientific research documents, whether they are published or not. The documents may come from teaching and research institutions in France or abroad, or from public or private research centers.

L'archive ouverte pluridisciplinaire **HAL**, est destinée au dépôt et à la diffusion de documents scientifiques de niveau recherche, publiés ou non, émanant des établissements d'enseignement et de recherche français ou étrangers, des laboratoires publics ou privés.

Distributed under a Creative Commons Attribution - NonCommercial 4.0 International License

Version of Record: https://www.sciencedirect.com/science/article/pii/S0022202X21021655
Manuscript_f29497ea3483a8f89f93348c2e507c42

Merkel cell polyomavirus-negative -Merkel cell carcinoma originating from *in situ* squamous cell carcinoma: a keratinocytic tumor with neuroendocrine differentiation

Thibault Kervarrec[1,2,3*,**], Silke Appenzeller[4**], Mahtab Samimi[2,5], Bhavishya Sarma[3], Eva-Maria Sarosi[3], Patricia Berthon[2], Yannick Le Corre[6], Ewa Hainaut-Wierzbicka[7] Astrid Blom[8], Nathalie Benethon[9], Guido Bens[10], Charline Nardin[11], Francois Aubin[11], Monica Dinulescu[12], Marie-Laure Jullie[13], Ágnes Pekár-Lukacs[14,15], Eduardo Calonje[15], Soumanth Thanguturi[1], Anne Tallet[16], Marion Wobser[3], Antoine Touzé[2], Serge Guyétant[1,2], Roland Houben[3***] & David Schrama[3***]

1 Department of Pathology, Université de Tours, Centre Hospitalier Universitaire de Tours, 37044 Tours, France
2 "Biologie des infections à polyomavirus" team, UMR INRAE ISP 1282, Université de Tours, 37200 Tours, France
3 Department of Dermatology, Venereology and Allergology, University Hospital Würzburg, 97080 Würzburg, Germany
4 Core Unit Bioinformatics, Comprehensive Cancer Center Mainfranken, University Hospital of Würzburg, 97080 Würzburg, Germany
5 Departement of Dermatology, Université de Tours, Centre Hospitalier Universitaire de Tours, 37044 Tours, France
6 Dermatology Department, LUNAM Université, CHU Angers, 49933 Angers, France
7 Dermatology Department, Université de Poitiers, CHU de Poitiers, 2 rue de la Milétrie, 86021 Poitiers, France
8 Department of General and Oncologic Dermatology, CARADERM networkAmbroise-Paré hospital, APHP & Research unit EA 4340, university of Versailles-Saint-Quentin-en-Yvelines, Paris-Saclay University, 92100, Boulogne-Billancourt France
9 Dermatology Department, CHR Le Mans, 194 avenue Rubillard 72037 Le Mans Cedex 09, France
10 Dermatology Department, CHR d'Orléans, 14 avenue de l'hôpital, 45100 Orléans, France
11 Dermatology Department, Université de Franche Comté, CHU Besançon, EA3181, IFR133, 2 boulevard Fleming 25030 Besançon, France
12 Dermatology Department, CHR Rennes, 2 rue Henri le Guilloux 35000 Rennes Cedex, France ; Institut Dermatologique du Grand Ouest (IDGO)
13 Department of Pathology, Hôpital Haut-Lévêque, CHU de Bordeaux, CARADERM network, 33604 Pessac, France
14 Department of Oncology and Pathology, Lund University, Lund, Sweden.
15 Department of Dermatopathology, St John's Institute of Dermatology, St Thomas's Hospital, Westminster Bridge Road, London, SE1 7EH, UK
16 Platform of Somatic Tumor Molecular Genetics, Université de Tours, Centre Hospitalier Universitaire de Tours, 37044 Tours, France

(*) T. Kervarrec is the corresponding author. (**) T. Kervarrec, and S. Appenzeller contributed equally to the present study. (***) D. Schrama and R. Houben contributed equally to the present study

Disclosure/Conflict of Interest: The authors declare no conflict of interest.

Grant numbers and sources of support: Fondation ARC pour la recherche contre le cancer, Interdisziplinäres Zentrum für Klinische Forschung Würzburg (IZKF B-343) and by the German Research Foundation (SCHR 1178/3-1). Ligue Nationale Contre le Cancer, Comités 16, 18, 28, HUGO Grant.

Institutional review board: The local Ethics Committee of Tours (France) approved the study (no. RCB2009-A01056-51)

Corresponding author:
Dr Thibault Kervarrec
Department of Pathology, Hôpital Trousseau, CHRU de Tours, 37044 TOURS Cedex 09 France. Tel: +33 (2) 47 47 80 69/Fax: +33 (2) 47 47 46 22
Email: thibaultkervarrec@yahoo.fr

Word count (Excluding abstract and references): 4064/Abstract: 154.
List of attachments: Figures: 4 / Table 1/ Supplements consisting of Tables: 4, Figures: 7 and Supplementary Materials: 2)

© 2021 published by Elsevier. This manuscript is made available under the CC BY NC user license
https://creativecommons.org/licenses/by-nc/4.0/

ORCID:

Thibault Kervarrec: https://orcid.org/0000-0002-2201-6914
Silke Appenzeller: https://orcid.org/0000-0002-5472-8692
Mahtab Samimi: https://orcid.org/0000-0001-6742-9088
Bhavishya Sarma: https://orcid.org/0000-0002-1262-4721
Eva-Maria Sarosi: https://orcid.org/0000-0001-5075-4685
Patricia Berthon: https://orcid.org/0000-0002-3491-7613
Yannick Le Corre: https://orcid.org/ 0000-0003-3089-3068
Ewa Hainaut-Wierzbicka: https://orcid.org/0000-0002-6475-4018
Astrid Blom: https://orcid.org/0000-0002-2848-3724
Nathalie Benethon: https//orcid.org/ 0000-0002-3052-2366
Monica Dinulesc: https://orcid.org /0000-0002-3950-4340
Francois Aubin: https://orcid.org /0000-0003-3171-8974
Charline Nardine: https://orcid.org /0000-0002-9902-5990
Marie-Laure Jullie: https://orcid.org/0000-0002-0048-6501
Ágnes Pekár-Lukacs: http://orcid.org: 0000-0001-7776-4744
Eduardo Calonje: https://orcid.org/0000-0001-7475-6423
Soumanth Thanguturi: https://orcid.org/0000-0001-6590-6805
Anne Tallet: https://orcid.org/0000-0002-2601-2443
Marion Wobser: https://orcid.org/0000-0002-6293-2554
Antoine Touzé: https://orcid.org/0000-0002-9856-9945
Serge Guyétant: https://orcid.org/0000-0003-2783-9722
David Schrama: https://orcid.org/0000-0002-6931-8194
Roland Houben: https://orcid.org/0000-0003-4538-2324

Abstract

While virus-negative Merkel cell carcinoma (MCC) is characterized by high frequency of UV-induced mutations, expression of two viral oncoproteins is regarded as key mechanism driving Merkel cell polyomavirus (MCPyV)-positive MCC. The cells in which these molecular events initiate MCC oncogenesis have yet not been identified for both MCC subsets. A considerable proportion of virus-negative MCC is found in association with squamous cell carcinoma (SCC) suggesting (i) coincidental collision, (ii) one providing a niche for the other or (iii) one evolving from the other. Whole exome sequencing of four combined tumors consisting of SCC *in situ* and MCPyV-negative MCC demonstrated in all cases many mutations shared between SCC and MCC indicating a common ancestry and thereby a keratinocytic origin of these MCCs. Moreover, analyses of the combined cases as well as of pure SCC and MCC suggests that RB1 inactivation in SCC facilitates MCC development and that epigenetic changes may contribute to the SCC/MCC transition.

Introduction

Merkel cell carcinoma (MCC), i.e. primary neuroendocrine carcinoma of the skin, is an aggressive skin neoplasm (Harms et al. 2018). In 2008, Feng et al. identified a beforehand unknown Merkel cell polyomavirus (MCPyV) integrated in the genome of MCC tumor cells (Feng et al. 2008). Further studies confirmed MCPyV integration in about 80% of cases, and demonstrated a crucial involvement of the two viral T antigens expressed in MCPyV-positive MCC, i.e. small T (sT) and large T (LT) antigen, in transformation and tumor cell proliferation (Harms et al. 2018). While sequestration of RB1 and subsequent E2F release appears as the main contribution of LT to MCC oncogenesis (Harms et al. 2018; Houben et al. 2012), sT affects cell biology via several mechanisms such as recruiting MYCL to the EP400 complex which subsequently leads to several downstream events like expression of the lysine specific histone demethylase (LSD1) and inactivation of p53 (Harms et al. 2018; Park et al. 2020). The 20% of MCC cases not associated with MCPyV are thought to be driven by DNA damage caused by UV exposure (Harms et al. 2015; Starrett et al. 2020). Indeed, high tumor mutational burden and UV-signature are hallmarks of virus-negative MCC (Goh et al. 2016; González-Vela et al. 2017; Harms et al. 2015).

Despite these advances in the understanding of the genetic background of MCC, the nature of the cells of origin remains to be determined, and might differ in the two subsets (Becker and Zur Hausen 2014; Harms et al. 2018; Kervarrec et al. 2019a; Sunshine et al. 2018; Zur Hausen et al. 2013). Indeed, while a transformation sequence of premalignant intraepithelial neoplasia to *in situ* and then invasive carcinoma is regarded as a rule for epithelial tumors (Ratushny et al. 2012; WHO 2018), no MCC precursor sequence has yet been clearly identified. This fact together with the dermal or subcutaneous location, lack of epidermal connection, and rare mutations in MCPyV-positive cases, has led some authors to propose a non-epidermal origin for the virus-associated MCC subtype (Harold et al. 2019; Sunshine et al. 2018).

By contrast, a high mutational load associated with UV signature characteristic for MCPyV-negative MCCs is normally restricted to cells in the most superficial layers of the skin (Sunshine et al. 2018). Moreover, virus-negative MCCs are frequently observed in close proximity to UV-related epithelial tumors, either evolving (actinic keratoses/carcinomas *in situ*) or established squamous cell carcinomas (Carter et al. 2018). The percentage of MCPyV-negative MCCs detected as tumors with combined SCC component are in the range of 10 to 38% of all MCC

cases (Ogawa et al. 2020; Walsh 2001). Although such co-localization might result from a common ancestry - and thereby suggesting virus-negative MCC as a keratinocytic cancer - it still remains a matter of debate, whether in combined SCC/MCC one component derives from the other (Carter et al. 2018; Falto Aizpurua et al. 2018).

Therefore, the main goal of the present study was to elucidate the relationship between the two components of co-occurring MCPyV-negative MCC and SCC. Indeed, whole exome sequencing of four squamous cell carcinoma *in situ* (SCCis) combined with MCC provided clear evidence that MCPyV-negative MCC can evolve from a keratinocytic tumor.

Results

Tested MCC cases associated with SCC*is* are not related to MCPyV oncogenesis.

To determine whether the MCC component in combined SCC/MCC might evolve from the associated SCC we choose four cases comprising SCC with an *in situ* component (SCC*is*) and invasive MCC because in case of a genetic relationship the direction of progression would be obvious. Clinical and microscopic features of the four cases are described in **Table 1/Figure 1**. With respect to etiology, several points argued for non-viral UV-mediated oncogenesis of the MCC part of the combined tumors: (i) prior clinical histories of multiple melanoma or non-melanoma skin cancers suggesting long-term UV exposure were identified in two cases, (ii) all tumors occurred in sun-exposed skin (head and neck: n=2, leg: n=2), and (iii) MCPyV is normally not detected in combined cases (Martin et al. 2013; Pulitzer et al. 2015).

Accordingly, microscopic features of MCC tumor cells were evocative of MCPyV-negative lesions with tumor cells displaying visible/clear cytoplasm in all cases (Iwasaki et al. 2013). Immunohistochemistry further revealed a so called “aberrant” profile with co-expression of MCC markers together with TTF-1 in three cases (Pasternak et al. 2018). In line with these observations, the lack of MCPyV was confirmed by immunohistochemistry and real time PCR in all cases (**Table 1**). Therefore, clinical, phenotypical and molecular characterization suggested non MCPyV-induced oncogenesis for all these combined tumors.

Interestingly, progressive cytological changes across the SCC*is* were observed in one specimen (case #2), and were most advanced in close proximity to the MCC part (**Supplementary Figure 1**). This continuous morphological spectrum from SCC*is* with successively decreasing

differentiation close to *in situ* and then invasive MCC might reflect the chronological course of tumor progression suggesting that an SCC cell gave rise to the MCC. This might be true for all investigated combined tumors since immunohistochemical detection of p53 revealed in all cases the same expression status in the respective SCC and MCC component (**Table 1/Supplementary Figure 2**) suggesting a common somatic alteration (Pulitzer et al. 2015).

High number of mutations shared between SCC*is* and the corresponding MCPyV-negative MCCs suggest common origin

In order to reveal a possible genetic relationship of the SCC and MCC components of the combined tumors, the two tumor parts of the four specimens were carefully dissected, followed by isolation of genomic DNA and whole exome sequencing. To detect somatic mutations, whole exome sequenced DNA derived from PBMCs or healthy tissue served as control **(Figure 2/Table 1/Supplementary Figure 3, Supplementary Tables 1-2).**

In line with the expected UV-mediated oncogenesis, for all samples, a high tumor mutational burden was evident by many somatic mutations present with an allelic frequency of ≥10%. For the SCC parts, an average of 760 (range: 172-1177) and for the MCC parts an average of 1173 (range: 436-2397) mutations could be detected. Moreover, mutation signature analyses confirmed prominent UV signature (COSMIC signature 7) in all cases and an additional APOPEC signature (COSMIC signature 13) for case 1 (**Supplementary Figure 4**) with similar mutational signature patterns for each part within a case confirming the likelihood of a shared origin of both components.

Importantly, a significant number of somatic variants (69-1060) were shared by both components of the same specimen (**Figure 2**). Notably, allelic frequencies of the shared variants in the MCC part were always higher than those observed in the SCC. In fact, the vast majority of frequencies were close to 50% in the MCC suggesting that the mutations shared with the respective SCC were heterozygously present in all MCC tumor cells given their tumor content of about 80%. In contrast, in the SCC parts shared mutations were detected with the majority of allelic frequencies ranging from 10 to 30% (Figure 2). Since - due to much more abundant stroma - the tumor cell content of the micro-dissected SCC parts ranged only from 30-50%, these mutational frequencies still translate into a presence of these somatic variants in most or all SCC cells (**Supplementary Figure 3 and Figure 2**). Accordingly, given the normal *in situ* to invasive tumor development sequence, these findings are in line with the scenario

that the invasive MCC part derived from the clonal expansion of an SCC tumor cell. Individual variants observed only in one tumor component, can be explained by their presence or absence in the specific MCC founder cell, thereby distinguishing this cell from those giving further rise to the finally observed SCC part. Alternatively, such mutations restricted to one tumor part may have appeared later in the natural history of the combined tumors. The common origin of both tumor components was further sustained by similar chromosomal alterations identified by copy number variation analyses (**Supplementary Figure 5**) and the before mentioned shared mutational signature pattern (**Supplementary Figure 4**).

No obvious genetic trigger for the SCC/MCC transition

Since our data demonstrated that MCPyV-negative MCC can derive from SCC*,* we then wondered whether we could identify genetic alterations which might contribute to the neuroendocrine transformation in the combined tumors. Thus, we searched for mutations specific for the MCC part. For this purpose, the most suitable of the four studied combined tumors was case #2 since only 40 mutations detected in the MCC were not shared with the corresponding SCC (**Figure 2**). Notably, 37 of these mutations were actually also present in the SCC component, but they did not pass our filter settings (**Supplementary Table 2**; category "MCC_and_below_filter_threshold_in_SCC") (see "somatic variant calling" in the methods section). Thus, only three mutations were truly restricted to the MCC component. The allelic frequencies of these variants of the *NACAD, PGGT1B* and *RLIM* gene were 51, 36 and 12%, respectively suggesting that all MCC cells are heterozygous for only the *NACAD* mutation while others occurred over time. This observation would be in accordance with a role as potential driver of MCC progression. However, NACAD is neither an established oncogene nor tumor suppressor, nor has any mutation in the coding sequence of *NACAD* been observed before in MCC (COSMIC data base). Therefore, the *NACAD* mutation is very unlikely to be crucial for MCC development. In conclusion, a potential genetic trigger for the SCC/MCC transition could not be identified in case #2.

The same is true for the three other combined tumors. Although the much higher number of MCC-specific alterations (**Figure 2**) increases the risk that a crucial genetic event has been overlooked, we were not able to detect established oncogenes or tumor suppressors among the proteins predicted to have an altered amino acid sequence only in the MCC part of the combined tumors. For a more systemic approach we analyzed the genes mutated in more

than one case and only present in the MCC compartment by DAVID for a functional annotation (Huang et al. 2009a; Huang et al. 2009b). To this end, for the 34 genes DAVID did only reveal a statistical significant enrichment for the keyword “guanine-nucleotide releasing factor”. The five genes ascribed to this group are *DOCK4*, *GAPDV1*, *HERC1*, *KALRN* and *PLEKHG1.* However, all these genes are characterized by a relatively large coding sequence (4158-14586 bp) increasing the likelihood of being bystander mutations in tumors with very high mutational burden. Moreover, for all five genes there was in addition to the two cases with restriction of the mutation to the MCC also always one case in which the mutation was present in both compartments. In conclusion it appears likely that none of these genetic alterations is responsible for the SCC/MCC transition.

Decreased histone methylation and acetylation distinguish MCC from SCC

If the SCC/MCC transition in the combined MCCs is not due to somatic mutations it might be caused by epigenetic changes. Moreover, we speculated that similar mechanisms might be operative in phenotype determination of MCPyV-positive and -negative MCC. In this respect, MCPyV-sT mediated induction of the lysine-specific demethylase 1 (LSD1) – an epigenetic modifier affecting histone methylation and acetylation – has recently been described as a key mechanisms in virus-induced MCC (Park et al. 2020). Therefore, we wondered whether changes in histone modifications might distinguish SCC from MCC. Although, not enough sufficient residual material of the four combined tumors for such an analysis, we addressed this question by immunohistochemical staining of a cohort of 173 pure MCC (42 MCPyV-negative and 131 MCPyV-positive) in comparison to a large series of non-MCC epithelial skin tumors (n=202) (**Figure 3**). Strikingly, strong and diffuse histone H3K4 mono-methylation and H3K27 acetylation was observed in almost all SCC, basal cell carcinoma (BCC) and skin appendage tumors while the majority of MCPyV-positive and MCPyV-negative MCCs displayed weak and heterogeneous staining (**Figure 3**). In conclusion, reduced histone H3K4 methylation and H3K27 acetylation are prominent features common between virus-positive and negative MCC, but distinguishes them from other epithelial skin tumors.

***RB1* inactivation and SOX2 expression might contribute to the SCC to MCC transformation.**

Since genetic alterations driving MCC development could not be identified we finally wondered whether molecular events predisposing SCC for progression to neuroendocrine

MCC can be identified. To this end, we determined all genes which were mutated with a considerable allelic frequency (≥ 40%) in the MCC component of at least two of our combined cases. For these genes (n=118; contains both potential driver like *TP53* and likely bystander mutations like *TTN*), we then extracted mutation frequencies from previously published whole exome sequencing data sets of MCPyV-negative MCC (n=43)(Goh et al. 2016; González-Vela et al. 2017; Harms et al. 2015) and cutaneous SCC (n=98) (Durinck et al. 2011; Li et al. 2015; Pickering et al. 2014; South et al. 2014; Uzilov et al. 2016; Yilmaz et al. 2017) (**Figure 4A/Supplementary Table 3**). Interestingly, similar mutation frequencies in SCC and MCC of most of these genes further support a possible common oncogenesis. Accordingly, for only 3 genes, there was an at least 2-fold mutation frequency increase in MCC compared to SCC (**Figure 4A**), and among them *RB1* displayed the highest MCC mutation rate (26 mutations/43 MCC cases (60%) vs 20 mutations/98 SCC cases (20%); $p=3.10^{-5}$, Fisher exact test). Notably, several genetic *RB1* aberrations were observed both in the MCC as well as in the SCC part of our combined tumors (**Table 1/Figure 4B**). Moreover, RB1 expression was lacking in both tumor components of all cases when assessed by immunohistochemistry (**Table 1/Supplementary Figure 2).**

Interestingly, it has recently been reported that RB1 inactivation can induce SOX2, a master regulator of Merkel cell development (Harold et al. 2019). In line with this, while only exceptionally rare cells in the normal epidermis (probably Merkel cells or melanocytes) expressed this transcription factor, strong SOX2 positivity was observed in both components of all combined SCC/MCC (**Figure 3C/Supplementary Figure 2**) suggesting that RB1 inactivation and SOX2 expression occurred before neuroendocrine transformation.

Notably, expression of SOX2 in all tumor cells appears to be a specific feature of the investigated SCCs giving rise to MCC, since it has been reported previously that in pure SCC SOX2 marks only a minor subset of tumor initiating cells (Siegle et al. 2014). To confirm this, we analyzed 24 pure cutaneous SCC and found that the majority (62.5%) completely lacked SOX2 while for the remaining weak and focal SOX2 staining was observed (**Supplementary Table 4/Supplementary Figure 6**). Moreover, RB1 staining demonstrated - again in contrast to the combined tumors - RB1 expression in the majority of pure SCCs (75%) (**Supplementary Table 4/Supplementary Figure 6**).

In conclusion, *RB1* inactivation and SOX2 expression appear as characteristic features of the SCC part of combined SCC/MCC. However, this inactivation likely constitutes an early mandatory but obviously not sufficient step towards development of MCPyV-negative MCC.

Discussion

Identification of the cellular origin of MCPyV-positive and -negative MCC is a high priority research objective not only to improve our understanding of MCC pathogenesis, but also to allow development of appropriate models which in turn can be utilized to develop new therapeutic options (Harms et al. 2018). In this context, although we recently demonstrated that MCPyV-positive MCC can arise from trichoblastoma (Kervarrec et al. 2020) suggesting an epithelial origin of MCPyV-positive MCC, lack of connection to the neighbouring epidermis, and lack of UV-signature argue for a non-epithelial origin of the virus associated subtype (Sunshine et al. 2018). In contrast, prominent UV-signature and frequent epidermal connection suggest a keratinocytic origin of MCPyV-negative MCC. Accordingly, by demonstrating that many somatic mutations are shared between both components of four combined SCC/MCC, and both compartments display similar CNV profiles and mutational signatures, our study presents compelling evidence for the keratinocytic origin of the MCC part of MCPyV-negative combined tumors. This may also be interpreted as further evidence for a keratinocytic origin of the more frequent pure MCC because highly similar genetic alterations and immunohistochemical profiles found in combined and pure MCPyV-negative tumors suggest that these two subsets represent one entity (Carter et al. 2018; Pasternak et al. 2018). One might speculate whether “pure” virus-negative MCC really arises *de novo* or whether a possible precursor lesion is only not detectable. Epidermal origin of all MCPyV-negative cases is further supported by exceptional cases of exclusively *in situ/*intraepidermal MCCs (**Supplementary Figure 7**).

While the master regulator of neuroendocrine differentiation SOX2 had - to the best of our knowledge - not been studied in MCPyV-negative MCC, data on its expression and function in the Merkel cell lineage and MCPyV-positive MCC are available. In this regard, expression of SOX2 in epidermal progenitors of healthy skin induces Merkel cell differentiation by up-regulating *Atonal homolog 1 (ATOH1)* gene transcription via direct binding to its promotor (Harold et al. 2019; Perdigoto et al. 2014). In MCPyV-positive tumor cells *SOX2* expression has been recently shown to support the neuroendocrine phenotype and its expression is dependent on Large T antigen inactivating RB1 (Harold et al. 2019). By comparing pure SCC with pure MCC we established that frequent *RB1* inactivation, is a prominent feature distinguishing MCPyV-negative MCC from SCC. Of note, a recent study investigating SCCis

genomic did not identify recurrent RB1 mutations in this setting (Zheng et al. 2021). Since RB1 inactivation and SOX2 expression were, however, observed in all SCC components of the combined tumors, we propose that *RB1* inactivation is a mandatory but not sufficient step for progression to MCC. Importantly, all four combined SCC/MCC tumors also harboured p53 mutations in both components. Therefore, a picture emerges which is reminiscent of small cell lung cancer, where concurrent RB1 and p53 alterations are almost always present (Su et al. 2019) and contribute to the neuroendocrine phenotype (Sutherland et al. 2011). In line with our observation, RB1 inactivation has been shown to define a subset of EGFR-mutant lung cancers at risk for histologic transformation to the neuroendocrine small cell type (Offin et al. 2019). Interestingly, Park and colleagues have demonstrated in experimental models that the same set of oncogenic drivers (MYC, BCL2, AKT as well as p53 and RB1 inactivation) can transform both normal lung and normal prostate epithelial cells into tissue specific neuroendocrine cancers (small cell prostate cancer and small cell lung cancer, respectively) (Park et al. 2018). Given our conclusion that MCPyV-negative MCC represents a neuroendocrine cancer that derives from cutaneous epithelial cells it is noteworthy that p53 and RB1 inactivation, AKT pathway activation (Hafner et al. 2012; Iwasaki et al. 2015), BCL2 expression (Vujic et al. 2015) and LMYC amplification (DeCaprio 2021; Paulson et al. 2009) have been reported as frequent events in these tumors suggesting analogues transformation processes.

We could not answer the intriguing question what finally causes the transition from SCC to MCC. Our data, however, suggest that this step can occur without additional genetic alterations, at least those we can identify by whole exome sequencing. A limitation of our study is that we were not able to rule out that fusions or copy number variation might be involved. Nevertheless, we identify reduced histone H3K4 methylation as a feature distinguishing MCC from classical keratinocytic tumors. H3K4 methylation represents a key mechanism for epigenetic regulation of gene expression and is controlled by the action of histone methyltransferases like KMT2D and the lysine-specific demethylase 1 (LSD1)(Morera et al. 2016). Mechanistically, KMT2D induced histone methylation activates while demethylation of mono- and di-methylated histone H3K4 by LSD1 represses gene transcription (Shi et al. 2004). Interestingly LSD1 activity has been recently identified as a specific vulnerability of MCPyV-positive MCC with inhibitors inducing differentiation and cell

death (Leiendecker et al. 2020; Park et al. 2020). In this regard it has been proposed that MCPyV-sT-induced induction of LSD1 is essential for growth of MCC cells by partially opposing the effect of ATOH1 to repress full differentiation (DeCaprio 2021; Park et al. 2020). Our observation that both virus-positive as well as virus-negative MCC can be distinguished from classical epithelial skin tumors by reduced H3K4-methylation (and the related H3K27-acetylation) allows the speculation that also in virus-negative MCC such a repression of growth-inhibiting full differentiation is essential for an MCC to develop (Alam et al. 2020; Dhar et al. 2018; Maitituoheti et al. 2020).

Conclusion:

Although, some authors propose MCPyV-negative and MCPyV-positive MCC to be two different entities (Nirenberg et al. 2020), the clinical and phenotypical overlap is still extensive. This may suggest that virus-positive and virus-negative MCC share similar cells of origin and that similar molecular events drive cancer development in both cases. Accordingly, the recent observation that virus-induced MCC can arise from trichoblastoma ((Kervarrec et al. 2020) and unpublished observation) indicates at least that an epithelial derivation is possible for MCPyV-positive MCC. An epithelial origin is also proposed for MCPyV-negative MCC (Nirenberg et al. 2020; Sunshine et al. 2018), and here we provide strong evidence that this is true for four virus-negative MCCs arising from SCC*is*. Moreover, our data also suggest *RB1* inactivation as a likely mandatory step for neuroendocrine differentiation of the tumor cells while reduced histone methylation may be important to allow further transition and growth of the tumor cells.

Material and Methods

Ethics

This study was approved by the local ethics committee (Tours, France, N° ID RCB2009-A01056-51), and written informed consent of the patients was obtained. Morphology and immunohistochemical profiles of two of the combined cases were previously published (Kervarrec et al. 2019b).

Immunohistochemistry

Immunohistochemical staining for CHGA, KRT5/6, KRT20, MCPyV-LT, RB1, TP53, and TTF-1 was

performed using a BenchMark XT Platform. Immunohistochemical staining for SOX2 was performed manually. Antibodies and dilutions are provided in **Supplementary Material**.

DNA isolation and MCPyV quantitative PCR

After microdissection of the two tumor components under a binocular magnifier, genomic DNA was isolated using the Maxwell 16 formalin-fixed and paraffin-embedded Plus LEV DNA purification kit (Promega). DNA from healthy tissue was obtained from peripheral blood mononuclear cells in 3 cases and from FFPE tissues adjacent to the tumor in one (case n°3). MCPyV status determination by real-time PCR was performed as previously described (Kervarrec et al. 2019b).

Next Generation Sequencing

For the exome library preparation, the SureSelectXT Library Prep Kit (Agilent) was used. Enrichment was performed using Agilent's SureSelectXT Human All Exon V6 Kit. The genomic library was prepared using TruSeq Nano DNA (Illumina). Paired-end sequencing with a read length of 100 bps (exomes) and 150 bps (genome) was performed on a NovaSeq 6000 (Illumina).

Data analysis

Demultiplexing of the sequencing reads was performed with Illumina bcl2fastq (v2.19). Adapters were trimmed with Skewer, v0.2.25. An initial quality assessment was performed using FastQC, v0.11.3 (Andrews S., 2010. Available online at: http://www.bioinformatics.babraham.ac.uk/projects/fastqc). Low-quality reads were trimmed with TrimGalore, v0.6.1 (Krueger, F., 2012: Available online at: http://www.bioinformatics.babraham.ac.uk/projects/trim_galore/) powered by Cutadapt, v2.3. The trimmed reads were mapped to the human reference genome (hg19) using BWA mem, v0.7.17 and sorted and indexed using Picard, v1.125 (available online at: http://broadinstitute.github.io/picard/) and SAMtools, v1.3 respectively. Duplicates were marked with Picard. Base recalibration was executed with GATK, v4.0.11.0. GATK, v3.59 was used for coverage calculations.

Somatic variant calling

MuTect2 (v4.0.11.0), VarScan2 (v2.4.1), Strelka2 (v2.9.2) and Scalpel (v0.5.3)were used to

identify somatic single nucleotide variants (SNVs) and small somatic insertions or deletions. We considered variants detected by two or more callers for downstream analysis. All variants were annotated with ANNOVAR, v2018-04-16. Variants were considered somatic if they have an impact on the protein sequence or affect a splice site, are rare in the population (below a frequency of 2% in 1000g2015aug_all, ExAC_nontcga_ALL, gnomAD_exome_ALL and gnomAD_genome_ALL) and the position is covered by at least 20 reads and the alternative allele is covered by at least 8 reads and comprises at least 10% of all reads. If a variant was detected in one tumor using the criteria mentioned above but failed other filter thresholds or was only called by one of the callers in the other tumor of the same patient we reported the variant and added the information "below threshold" to the last column (**Supplementary Table 2**).

For Venn diagrams and violin plots of mutation frequency only mutations with >=10% were considered. Mutational signatures were identified using MutaGene. For this analysis synonymous variants were also included .

CNV analysis

Somatic Copy Number Variations (CNVs) were called with VarScan2 (v2.4.1). All references for bioinformatic tools used are available in **Supplementary Methods**.

Data availability statement

The datasets generated during and/or analysed during the current study will be available in European Genome-phenome Archive: EGAS00001005028-.

Analysis of previously published data sets

Previous studies including investigation of MCPyV-negative MCC or cutaneous SCC by whole exome sequencing were identified from COSMIC and Medline database. The number of mutations/samples were extracted from COSMIC or from the studies presented in the supplementary files.

CRediT statement:

Conceptualization: TK, SA, RH, DS, MS, SG and AT ; Data curation: TK, SA, RH, DS; Formal Analysis: TK, SA, RH, DS, MS, SG and AT; Writing: TK, SA, RH, DS, formal analysis : TK, SA, RH, DS, MS, BS, ES, PB, YL, AB, NB, GB, CN, FA, MD, MJ, AP, EC, ST, AT, Methodology: MS, SG and AT, ressources: MS, SG, AT, DS, Investigation : BS, ES, PB, YL, AB, NB, GB, CN, FA, MD, MJ, AP, EC, ST, AT investigation, Manuscript revision : all.

References

Alam H, Tang M, Maitituoheti M, Dhar SS, Kumar M, Han CY, et al. KMT2D Deficiency Impairs Super-Enhancers to Confer a Glycolytic Vulnerability in Lung Cancer. Cancer Cell. 2020;37(4):599-617.e7

Becker JC, Zur Hausen A. Cells of origin in skin cancer. J. Invest. Dermatol. 2014;134(10):2491–3

Carter MD, Gaston D, Huang W-Y, Greer WL, Pasternak S, Ly TY, et al. Genetic profiles of different subsets of Merkel cell carcinoma show links between combined and pure MCPyV-negative tumors. Hum. Pathol. 2018;71:117–25

Chen C, Liu Y, Rappaport AR, Kitzing T, Schultz N, Zhao Z, et al. MLL3 is a haploinsufficient 7q tumor suppressor in acute myeloid leukemia. Cancer Cell. 2014;25(5):652–65

DeCaprio JA. Molecular Pathogenesis of Merkel Cell Carcinoma. Annu. Rev. Pathol. 2021;16:69–91

Dhar SS, Zhao D, Lin T, Gu B, Pal K, Wu SJ, et al. MLL4 Is Required to Maintain Broad H3K4me3 Peaks and Super-Enhancers at Tumor Suppressor Genes. Mol. Cell. 2018;70(5):825-841.e6

Durinck S, Ho C, Wang NJ, Liao W, Jakkula LR, Collisson EA, et al. Temporal dissection of tumorigenesis in primary cancers. Cancer Discov. 2011;1(2):137–43

Falto Aizpurua LA, Wang M, Ruiz HA, Sánchez JL, Chan MP, Andea AA, et al. A case of combined Merkel cell carcinoma and squamous cell carcinoma: Molecular insights and diagnostic pitfalls. JAAD Case Rep. 2018;4(10):996–9

Feng H, Shuda M, Chang Y, Moore PS. Clonal integration of a polyomavirus in human Merkel cell carcinoma. Science. 2008;319(5866):1096–100

Froimchuk E, Jang Y, Ge K. Histone H3 lysine 4 methyltransferase KMT2D. Gene. 2017;627:337–42

Goh G, Walradt T, Markarov V, Blom A, Riaz N, Doumani R, et al. Mutational landscape of MCPyV-positive and MCPyV-negative Merkel cell carcinomas with implications for immunotherapy. Oncotarget. 2016;7(3):3403–15

González-Vela MDC, Curiel-Olmo S, Derdak S, Beltran S, Santibañez M, Martínez N, et al. Shared Oncogenic Pathways Implicated in Both Virus-Positive and UV-Induced Merkel Cell Carcinomas. J. Invest. Dermatol. 2017;137(1):197–206

Hafner C, Houben R, Baeurle A, Ritter C, Schrama D, Landthaler M, et al. Activation of the PI3K/AKT pathway in Merkel cell carcinoma. PloS One. 2012;7(2):e31255

Harms PW, Harms KL, Moore PS, DeCaprio JA, Nghiem P, Wong MKK, et al. The biology and treatment of Merkel cell carcinoma: current understanding and research priorities. Nat. Rev. Clin. Oncol. 2018;15(12):763–76

Harms PW, Vats P, Verhaegen ME, Robinson DR, Wu Y-M, Dhanasekaran SM, et al. The Distinctive Mutational Spectra of Polyomavirus-Negative Merkel Cell Carcinoma. Cancer Res. 2015;75(18):3720–7

Harold A, Amako Y, Hachisuka J, Bai Y, Li MY, Kubat L, et al. Conversion of Sox2-dependent Merkel cell carcinoma to a differentiated neuron-like phenotype by T antigen inhibition. Proc. Natl. Acad. Sci. U. S. A. 2019;

Houben R, Adam C, Baeurle A, Hesbacher S, Grimm J, Angermeyer S, et al. An intact retinoblastoma protein-binding site in Merkel cell polyomavirus large T antigen is required for promoting growth of Merkel cell carcinoma cells. Int. J. Cancer. 2012;130(4):847–56

Huang DW, Sherman BT, Lempicki RA. Bioinformatics enrichment tools: paths toward the comprehensive functional analysis of large gene lists. Nucleic Acids Res. 2009a;37(1):1–13

Huang DW, Sherman BT, Lempicki RA. Systematic and integrative analysis of large gene lists using DAVID bioinformatics resources. Nat. Protoc. 2009b;4(1):44–57
Iwasaki T, Matsushita M, Kuwamoto S, Kato M, Murakami I, Higaki-Mori H, et al. Usefulness of significant morphologic characteristics in distinguishing between Merkel cell polyomavirus-positive and Merkel cell polyomavirus-negative Merkel cell carcinomas. Hum. Pathol. 2013;44(9):1912–7
Iwasaki T, Matsushita M, Nonaka D, Kuwamoto S, Kato M, Murakami I, et al. Comparison of Akt/mTOR/4E-BP1 pathway signal activation and mutations of PIK3CA in Merkel cell polyomavirus-positive and Merkel cell polyomavirus-negative carcinomas. Hum. Pathol. 2015;46(2):210–6
Kervarrec T, Aljundi M, Appenzeller S, Samimi M, Maubec E, Cribier B, et al. Polyomavirus-Positive Merkel Cell Carcinoma Derived from a Trichoblastoma Suggests an Epithelial Origin of this Merkel Cell Carcinoma. J. Invest. Dermatol. 2020;140(5):976–85
Kervarrec T, Samimi M, Guyétant S, Sarma B, Chéret J, Blanchard E, et al. Histogenesis of Merkel cell carcinoma: a comprehensive review. Front. Oncol. Accepted Manuscript. 2019a;
Kervarrec T, Tallet A, Miquelestorena-Standley E, Houben R, Schrama D, Gambichler T, et al. Morphologic and immunophenotypical features distinguishing Merkel cell polyomavirus-positive and -negative Merkel cell carcinoma. Mod. Pathol. Off. J. U. S. Can. Acad. Pathol. Inc. 2019b;
Leiendecker L, Jung PS, Krecioch I, Neumann T, Schleiffer A, Mechtler K, et al. LSD1 inhibition induces differentiation and cell death in Merkel cell carcinoma. EMBO Mol. Med. 2020;12(11):e12525
Li YY, Hanna GJ, Laga AC, Haddad RI, Lorch JH, Hammerman PS. Genomic analysis of metastatic cutaneous squamous cell carcinoma. Clin. Cancer Res. Off. J. Am. Assoc. Cancer Res. 2015;21(6):1447–56
Maitituoheti M, Keung EZ, Tang M, Yan L, Alam H, Han G, et al. Enhancer Reprogramming Confers Dependence on Glycolysis and IGF Signaling in KMT2D Mutant Melanoma. Cell Rep. 2020;33(3):108293
Martin B, Poblet E, Rios JJ, Kazakov D, Kutzner H, Brenn T, et al. Merkel cell carcinoma with divergent differentiation: histopathological and immunohistochemical study of 15 cases with PCR analysis for Merkel cell polyomavirus. Histopathology. 2013;62(5):711–22
Morera L, Lübbert M, Jung M. Targeting histone methyltransferases and demethylases in clinical trials for cancer therapy. Clin. Epigenetics. 2016;8:57
Nirenberg A, Steinman H, Dixon J, Dixon A. Merkel cell carcinoma update: the case for two tumours. J. Eur. Acad. Dermatol. Venereol. JEADV. 2020;34(7):1425–31
Offin M, Chan JM, Tenet M, Rizvi HA, Shen R, Riely GJ, et al. Concurrent RB1 and TP53 Alterations Define a Subset of EGFR-Mutant Lung Cancers at risk for Histologic Transformation and Inferior Clinical Outcomes. J. Thorac. Oncol. Off. Publ. Int. Assoc. Study Lung Cancer. 2019;14(10):1784–93
Ogawa T, Donizy P, Wu C-L, Cornejo KM, Ryś J, Hoang MP. Morphologic Diversity of Merkel Cell Carcinoma. Am. J. Dermatopathol. 2020;42(9):629–40
Ortega-Molina A, Boss IW, Canela A, Pan H, Jiang Y, Zhao C, et al. The histone lysine methyltransferase KMT2D sustains a gene expression program that represses B cell lymphoma development. Nat. Med. 2015;21(10):1199–208
Park DE, Cheng J, McGrath JP, Lim MY, Cushman C, Swanson SK, et al. Merkel cell polyomavirus activates LSD1-mediated blockade of non-canonical BAF to regulate transformation and tumorigenesis. Nat. Cell Biol. 2020;
Park JW, Lee JK, Sheu KM, Wang L, Balanis NG, Nguyen K, et al. Reprogramming normal human epithelial tissues to a common, lethal neuroendocrine cancer lineage. Science. 2018;362(6410):91–5

Pasternak S, Carter MD, Ly TY, Doucette S, Walsh NM. Immunohistochemical profiles of different subsets of Merkel cell carcinoma. Hum. Pathol. 2018;82:232–8
Paulson KG, Lemos BD, Feng B, Jaimes N, Peñas PF, Bi X, et al. Array-CGH reveals recurrent genomic changes in Merkel cell carcinoma including amplification of L-Myc. J. Invest. Dermatol. 2009;129(6):1547–55
Perdigoto CN, Bardot ES, Valdes VJ, Santoriello FJ, Ezhkova E. Embryonic maturation of epidermal Merkel cells is controlled by a redundant transcription factor network. Dev. Camb. Engl. 2014;141(24):4690–6
Pickering CR, Zhou JH, Lee JJ, Drummond JA, Peng SA, Saade RE, et al. Mutational landscape of aggressive cutaneous squamous cell carcinoma. Clin. Cancer Res. Off. J. Am. Assoc. Cancer Res. 2014;20(24):6582–92
Pulitzer MP, Brannon AR, Berger MF, Louis P, Scott SN, Jungbluth AA, et al. Cutaneous squamous and neuroendocrine carcinoma: genetically and immunohistochemically different from Merkel cell carcinoma. Mod. Pathol. Off. J. U. S. Can. Acad. Pathol. Inc. 2015;28(8):1023–32
Ratushny V, Gober MD, Hick R, Ridky TW, Seykora JT. From keratinocyte to cancer: the pathogenesis and modeling of cutaneous squamous cell carcinoma. J. Clin. Invest. 2012;122(2):464–72
Shi Y, Lan F, Matson C, Mulligan P, Whetstine JR, Cole PA, et al. Histone demethylation mediated by the nuclear amine oxidase homolog LSD1. Cell. 2004;119(7):941–53
Siegle JM, Basin A, Sastre-Perona A, Yonekubo Y, Brown J, Sennett R, et al. SOX2 is a cancer-specific regulator of tumour initiating potential in cutaneous squamous cell carcinoma. Nat. Commun. 2014;5:4511
South AP, Purdie KJ, Watt SA, Haldenby S, den Breems N, Dimon M, et al. NOTCH1 mutations occur early during cutaneous squamous cell carcinogenesis. J. Invest. Dermatol. 2014;134(10):2630–8
Starrett GJ, Thakuria M, Chen T, Marcelus C, Cheng J, Nomburg J, et al. Clinical and molecular characterization of virus-positive and virus-negative Merkel cell carcinoma. Genome Med. 2020;12(1):30
Su S, Zou J-J, Zeng Y-Y, Cen W-C, Zhou W, Liu Y, et al. Tumor Mutational Burden and Genomic Alterations in Chinese Small Cell Lung Cancer Measured by Whole-Exome Sequencing. BioMed Res. Int. 2019;2019:6096350
Sunshine JC, Jahchan NS, Sage J, Choi J. Are there multiple cells of origin of Merkel cell carcinoma? Oncogene. 2018;37(11):1409–16
Sutherland KD, Proost N, Brouns I, Adriaensen D, Song J-Y, Berns A. Cell of origin of small cell lung cancer: inactivation of Trp53 and Rb1 in distinct cell types of adult mouse lung. Cancer Cell. 2011;19(6):754–64
Uzilov AV, Ding W, Fink MY, Antipin Y, Brohl AS, Davis C, et al. Development and clinical application of an integrative genomic approach to personalized cancer therapy. Genome Med. 2016;8(1):62
Vujic I, Marker M, Posch C, Mühlehner D, Monshi B, Breier F, et al. Merkel cell carcinoma: mitoses, expression of Ki-67 and bcl-2 correlate with disease progression. J. Eur. Acad. Dermatol. Venereol. JEADV. 2015;29(3):542–8
Walsh NM. Primary neuroendocrine (Merkel cell) carcinoma of the skin: morphologic diversity and implications thereof. Hum. Pathol. 2001;32(7):680–9
WHO. WHO classification of skin tumours. 4th edition. Elder DE, Massi D, Scolyer RA, Willemze R, editors. Lyon: International Agency for Research on Cancer; 2018.
Yilmaz AS, Ozer HG, Gillespie JL, Allain DC, Bernhardt MN, Furlan KC, et al. Differential mutation frequencies in metastatic cutaneous squamous cell carcinomas versus primary tumors. Cancer. 2017;123(7):1184–93

Zheng Q, Capell BC, Parekh V, O'Day C, Atillasoy C, Bashir HM, et al. Whole-Exome and Transcriptome Analysis of UV-Exposed Epidermis and Carcinoma In Situ Reveals Early Drivers of Carcinogenesis. J. Invest. Dermatol. 2021;141(2):295-307.e13
Zur Hausen A, Rennspiess D, Winnepenninckx V, Speel E-J, Kurz AK. Early B-cell differentiation in Merkel cell carcinomas: clues to cellular ancestry. Cancer Res. 2013;73(16):4982–7

Figure 1. Microscopic and immunohistochemical features of the SCC*is*/MCC combined tumors. A. Morphological features of the four cases (hematein-phloxin-saffron staining (HPS), bars are 100µm and 2mm respectively). The SCC parts were composed of an *in situ* and sometimes invasive (cases 1 and 3) carcinomatous proliferations of tumor cells harboring abundant, sometimes clear cytoplasm and hyperchromatic enlarged nucleus with prominent nucleoli. By contrast, higher nucleocytoplasmic ratios with coarse hyperchromatic chromatin were observed in the MCC parts. **B. Immunohistochemical details of case n°3**. While the SCC part was characterized by expression of the cytokeratins (KRT) 5/6, positivity of KRT20, and of the neuroendocrine marker chromogranine A (CHGA) were restricted to the MCC component. Weak expression of TTF-1 was also observed in the MCC part which lacked expression of KRT7.

Figure 2. SCC and MCC cells of the combined tumor share pathologic somatic variants. Venn diagrams demonstrating the overlap of mutations between SCC*is* and MCC. Allelic frequencies of the non-synonymous variants specific to the respective parts (individual) or shared are presented by violin plots.

Figure 3. Histone H3K27 acetylation and H3K4 mono methylation levels in MCC and non MCC epithelial skin tumors. A. Histone H3K27 acetylation level in MCC and non MCC epithelial skin tumors. **B.** Histone H3K4 methylation level in MCC and non MCC epithelial skin tumors. **C.** representative illustration of Histone H3K27 acetylation and H3K4 methylation levels in the

SCC and MCC part of one combined SCC/MCC (case #1). (Bar indicates 100 µm). Non MCC tumors consisted in 73 squamous cell carcinoma, 31 basal cell carcinoma, 11 spiradenoma, 10 poroma, 10 trichoblastoma, 9 sebaceous adenoma, 9 hidradenoma, 7 mixed tumors, 6 Paget diseases, 5 trichilemmoma, 4 pilomatricoma, 4 trichoepithelioma, 3 poroid hidradenoma, 3 adnexal adenocarcinoma not otherwise specified, 3 proliferating trichilemmal cysts, 2 primary cutaneous mucinous carcinoma, 2 adenoid cystic carcinoma, 2 sebaceous carcinoma, 2 cylindroma, 2 myoepithelioma, 1 pilomatrical carcinoma, 1 porocarcinoma. Only cases with interpretable staining were taking account.

Figure 4. *RB1* inactivation might contribute to promote neuroendocrine differentiation in SCC. A. Mutation frequencies in previously published data sets of SCC and MCC. Mutation frequencies of selected genes (n=118; **Supplementary Table 3)** were extracted from previously published data sets of MCPyV-negative MCC (n=43) and cutaneous SCC (n=98). The results as mutation-number/100 cases are depicted for 50 most common mutated genes in MCC. **B. RB1 alteration in the four combined cases.** Mutations/LOH are depicted for cases 1 (yellow), 2 (black), 3 (red) and 4 (blue) (CYCA/B: Cyclin fold A/B domain, PA/B: Pocket domain A/B)**. C. Immunohistochemical detection of SOX2 in a combined case** (case 2, bar = 2.5mm)**.** SOX2 expression was almost completely restricted to both tumor components with higher expression in the MCC part.

Table 1 Clinical and microscopic features of the 4 combined cases.

Clinical features	Case 1		Case 2		Case 3		Case 4	
Age	80		83		81		75	
Sex	F		F		F		F	
Immunosuppression	No		No		No		Yes	
Previous skin cancers	-		1 Melanoma, 10 BCC, 1 AK		1 AK, 2 SCC		-	
Tumor location	Leg		Face		Leg		Neck	
AJCC stage	I		I		I		III	
Follow-up								
Duration, months	7		15		17		12	
Metastasis	Yes		Yes		Yes		Yes	
Death	Yes		No		Yes		No	
Immunomorphologic and virologic features	**Case 1**		**Case 2**		**Case 3**		**Case 4**	
	SCC	**MCC**	**SCC**	**MCC**	**SCC**	**MCC**	**SCC**	**MCC**
Tumor components								
In situ	+	-	+	+	+	-	+	-
Invasive	+	+	-	+	+	+	-	+
MCC markers								
Cytokeratin 20	-	++	-	++	-	++	-	++
Chromogranin A	-	++	-	++	-	++	-	-
Synaptophysin	-	++	-	++	-	++	-	++
CD56	-	++	-	++	-	NA	-	++
Other investigated markers								
TTF-1	-	+	-	+	-	+	-	-
P53	-	-	-	-	++	++	++	++
RB1	-	-	-	-	-	-	-	-
SOX2	+	++	+	++	+	++	+	++
MCPyV-LT	-	-	-	-	-	-	-	-
H3K27 acetylation	+	++	NA	NA	++	++	NA	NA
H3K4me1	+	++	NA	NA	++	++	NA	NA
MCPyV qPCR	No amplification		No amplification		No amplification		No amplification	
Genetic features[1]	**Case 1**		**Case 2**		**Case 3**		**Case 4**	
Genes and allelic freq., [%]	**SCC**	**MCC**	**SCC**	**MCC**	**SCC**	**MCC**	**SCC**	**MCC**
TP53 (NM_000546.4)	p.P20fs 46.8	95.5	r.spl 34.3 p.P19T 31.3	78.5 84.4	p.C238R 13	71.1	p.R248L 24.8	76.4
RB1 (NM 000321.2)	p.S249* 55.9 p.E365Q 37.8	92.6 35.7	-		p.R255* 13.2	56.8	p.G86* 3.0[$]	35.5
KMT2D (NM_003482.3)	p.Q3913* 25.0[$]	44.8	p.P4925S 17.1[$] p.H3178P 26.5	42.1 42.5	p.R4536* 17.5[$]	73.5	p.E2351* 15.9[$]	68.1
NOTCH1 (NM_017617.3)	-		p.N314S 49.2 p.P110L 49.3	89.8 87.3	-		p.P1231L -	39
KDR	-		p.V641L		-		-	

(NM_002253.2)				21.1	39.6			
				p.G493E				
				23.8	50.8			
PIK3C2B	p.L874V		-		p.T1351I		-	
(NM_002646.3)	14.8	29.6			-	24.6		

BCC: basal cell carcinoma, AK: actinc keratosis, NA: not available data, Nonfrsb : non frameshift substitution , SCC: squamous cell carcinoma, Spl: splicing, - lack, + weak/heterogeneous, ++strong and diffuse immunohistochemical expression, [1]: the mutation status of the 10 genes previously identified as the most common mutated genes in MCC are depicted (Starrett et al. 2020). To note no mutation were observed in *NOTCH2, ROS1, ARID1A* and *TSC1.* [$]: although these variants were below the detection threshold as described in the methods section, manual IGV-analysis allowed their identification.

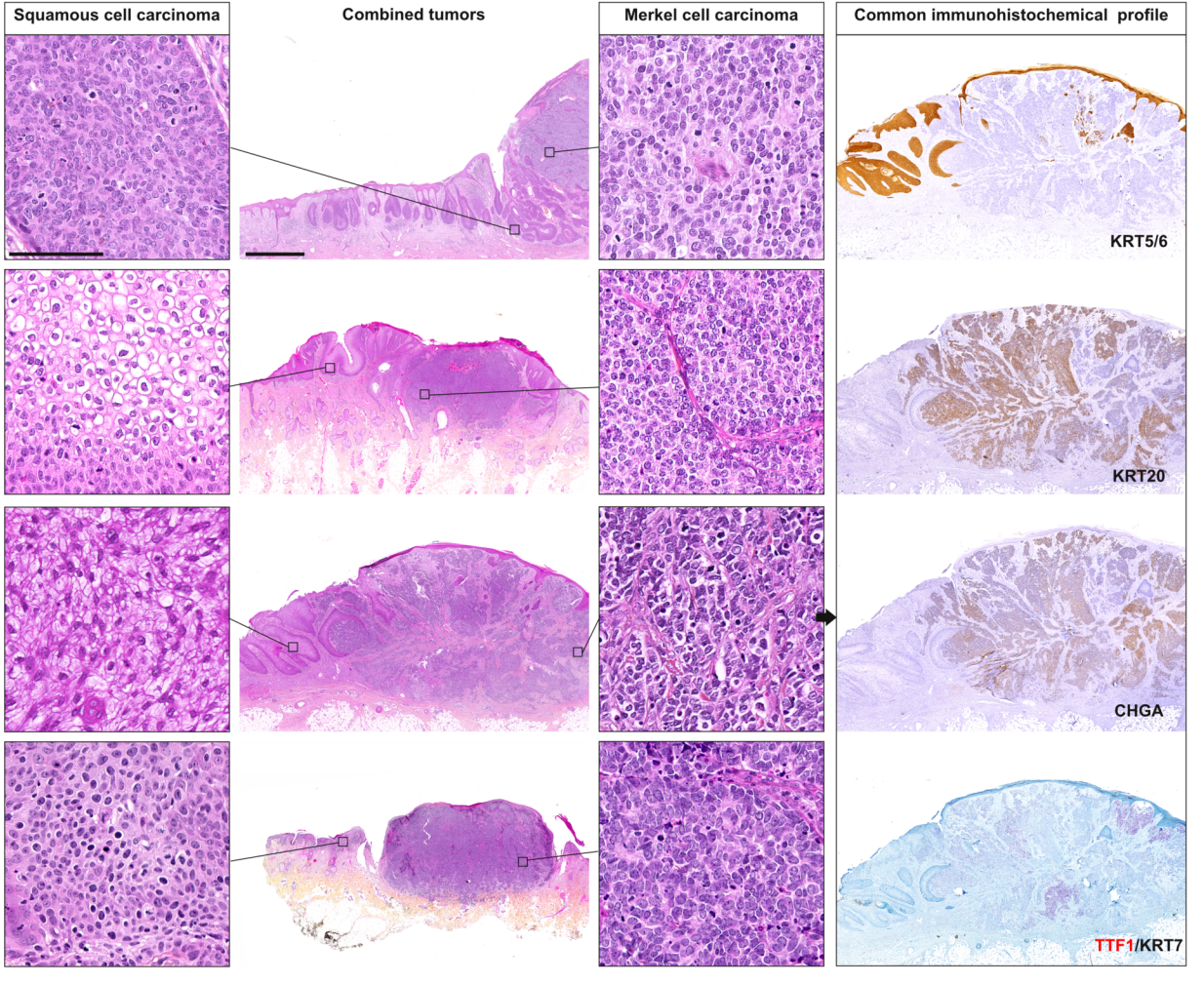
Squamous cell carcinoma
Combined tumors
Merkel cell carcinoma
Common immunohistochemical profile
KRT5/6
KRT20
CHGA
TTF1/KRT7

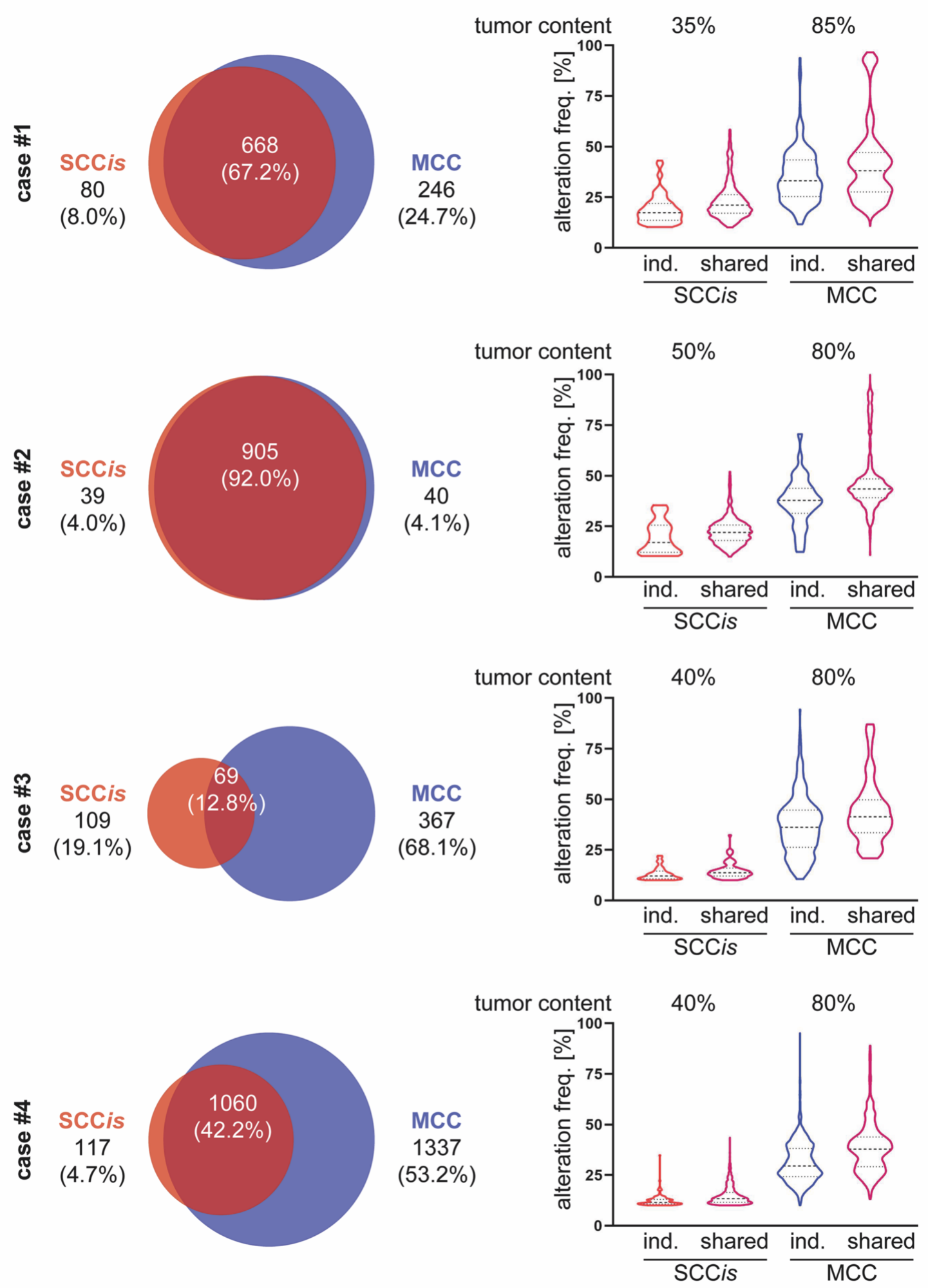
case #1
SCCis
80
(8.0%)
668
(67.2%)
MCC
246
(24.7%)
tumor content
35%
85%
alteration freq. [%]
100
75
50
25
0
ind.
shared
ind.
shared
SCCis
MCC
case #2
SCCis
39
(4.0%)
905
(92.0%)
MCC
40
(4.1%)
tumor content
50%
80%
alteration freq. [%]
100
75
50
25
0
ind.
shared
ind.
shared
SCCis
MCC
case #3
SCCis
109
(19.1%)
69
(12.8%)
MCC
367
(68.1%)
tumor content
40%
80%
alteration freq. [%]
100
75
50
25
0
ind.
shared
ind.
shared
SCCis
MCC
case #4
SCCis
117
(4.7%)
1060
(42.2%)
MCC
1337
(53.2%)
tumor content
40%
80%
alteration freq. [%]
100
75
50
25
0
ind.
shared
ind.
shared
SCCis
MCC

a

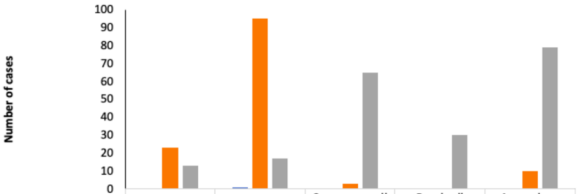

	MCPyV(-) MCC	MCPyV(+) MCC	Squamous cell carcinoma	Basal cell carcinoma	Appendage tumors*
Absent	0	1	0	0	0
Low/heterogeneous	23	95	3	0	10
High and diffuse	13	17	65	30	79

H3K27 acetylation level

b

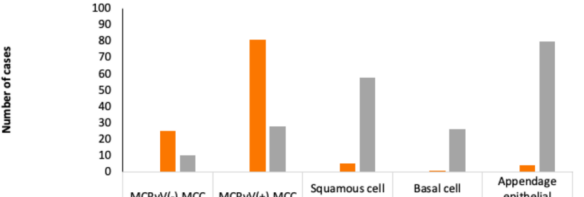

	MCPyV(-) MCC	MCPyV(+) MCC	Squamous cell carcinoma	Basal cell carcinoma	Appendage epithelial tumors*
Absent	0	0	0	0	0
Low/heterogeneous	25	81	5	1	4
High and diffuse	10	28	58	26	80

H3K4me1 methylation level

c

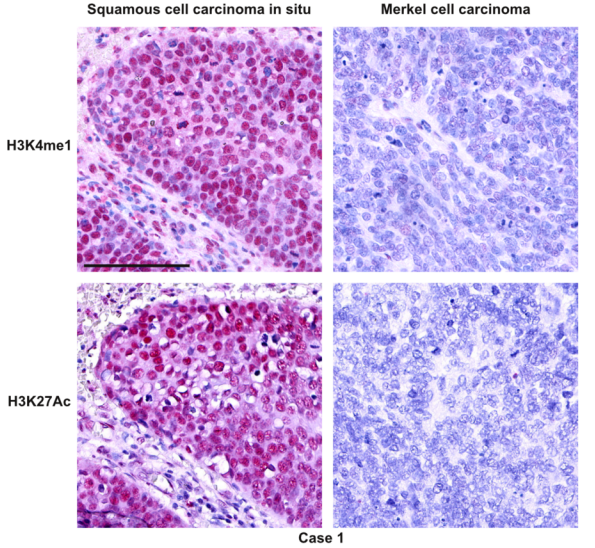

a

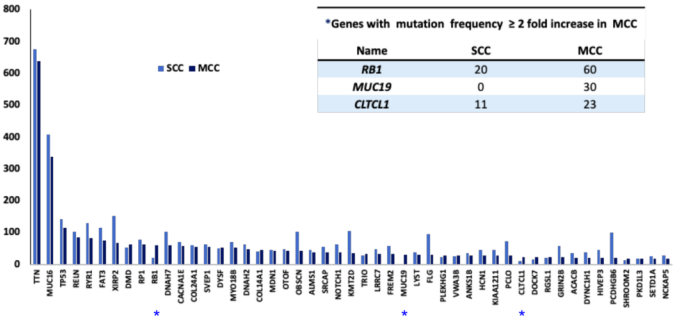

*Genes with mutation frequency ≥ 2 fold increase in MCC

Name	SCC	MCC
RB1	20	60
MUC19	0	30
CLTCL1	11	23

b

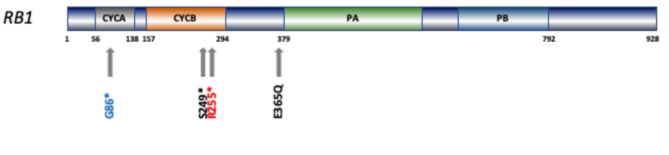
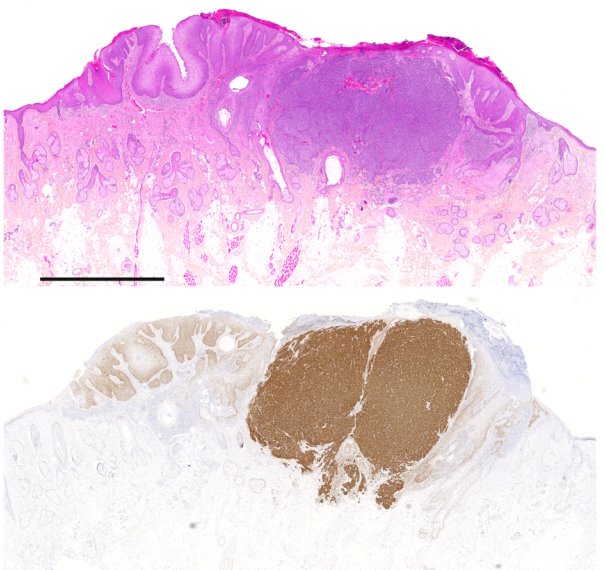
c